ORCSIM: A GENERALIZED ORGANIC RANKINE CYCLE SIMULATION TOOL

Davide Ziviani[1*], Brandon J. Woodland[2], Emeline Georges[3], Eckhard A. Groll, James E. Braun[2], W. Travis Horton[2], Michel De Paepe[1], Martijn van den Broek[1]

[1] Gent University, Department of Flow, Heat and Combustion Mechanics,
Gent, Belgium
davide.ziviani@ugent.be, michel.depaepe@ugent.be, martijn.vandenbroek@ugent.be

[2] Purdue University, School of Mechanical Engineering, Ray W. Herrick Laboratories,
West Lafayette, Indiana, U.S.A.
bwoodlan@purdue.edu, groll@purdue.edu, jbraun@purdue.edu, wthorton@purdue.edu

[3] University of Liege, Aerospace and mechanical Engineering Department, Energy Systems,
Liege, Belgium
emeline.georges@ulg.ac.be

* Corresponding Author

ABSTRACT

An increasing interest in organic Rankine cycle (ORC) technology has led to numerous simulation and optimization studies. In the open-literature different modeling approaches can be found, but general software tools available to the academic/industrial community are limited. A generalized ORC simulation tool, named ORCSim, is proposed in this paper. The framework is developed using object-oriented programming that easily allows improvements and future extensions. Currently two cycle configurations are implemented, i.e. a basic ORC and an ORC with liquid-flooded expansion. The software architecture, the thermo-physical property wrappers, the component library and the solution algorithm are discussed with particular emphasis on the ORC with liquid-flooded expansion. A thorough validation both at component and cycle levels is proposed by considering the aforementioned cycle architectures.

1. INTRODUCTION

An Organic Rankine cycle (ORC) is considered one of the most suitable systems to recover waste heat as well as to exploit renewable heat sources such as solar and geothermal. Although the technology is known, the optimization of such a system remains a key focus of ongoing research. Fluid selection, characterization of the cycle components and overall cycle analyses are a few of the common areas that researchers continue to explore (Quoilin et al., 2010; Woodland et al., 2014). In this context, a general ORC simulation framework, called ORCSim, is proposed to analyze such systems both at component and cycle levels. The cycle simulation is composed of a library of detailed models of each of the system components. While the general layout of the simulation tool and a brief introduction to the models of the components are outlined in Ziviani et al. (2015b), the present work focuses on a demonstration of the versatility of the tool. It can be applied to systems operating with different components, different working fluids and different hot/cold sources. Two ORC system architectures are considered in order to carry out a thorough validation, i.e. a standard ORC running with R245fa and an ORC with liquid-flooded expansion and internal regeneration, with R134a as the working fluid. In particular, the plate heat exchanger and expander models are described in detail because they present the highest level of complexity among the cycle components. An individual validation of these component models is also presented. The cycle simulation algorithm is explained along with the thermo-physical property routines. Finally, cycle simulations are carried out to validate the tool against experimental data.

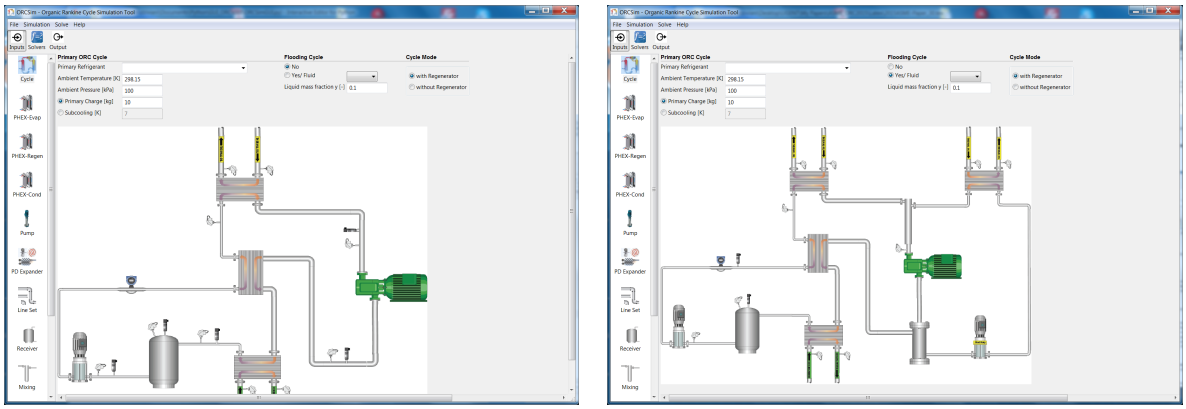

(a) (b)

Figure 1: (a) **ORC;**(b) **ORCLFE.**

2. ORCSIM ARCHITECTURE

ORCSim is a Python-based simulation tool which takes full advantage of the object-oriented programming environment. Its architecture and solution scheme were originally derived from the open source software for air conditioners and heat pumps, ACHP[1]. The first adaptation into an ORC simulation tool can be found in Georges (2012). The modularity of the code results in a flexible tool which allows the user to select not only the cycle configuration but also the desired type of model for each component. The graphical user interface (GUI) is shown in Fig. 1. Two cycle architectures are currently available and both are limited to subcritical applications: (i) standard organic Rankine cycle with/without internal regeneration, Fig. 1(a); (ii) organic Rankine cycle with liquid-flooded expansion and internal regeneration (Woodland et al., 2013), Fig. 1(b). The details of the GUI are described in Ziviani et al. (2015b).

2.1 Thermo-physical properties

In order to cover several ORC applications, the working fluid library has to be extensive, including both pure or pseudo-pure fluids as well as mixtures. Furthermore, many applications require thermal oils or other liquid heat transfer fluids to serve as the ORC heat source. The open-source thermo-physical property library CoolProp (Bell et al., 2014) has been used as the main source to retrieve properties for the wide range of refrigerants and incompressible fluids that may be used in ORC applications. This library implements the most accurate equations of state available in the literature, as well as highly efficient tabular interpolation methods to speed up property calculations. CoolProp can also be used as an interface layer around REFPROP (Lemmon et al., 2013). In this way, it is possible to make use of most of the features implemented in REFPROP as well as in CoolProp. A separate routine has been developed to compute the properties of the flooding mediums, typically lubricant oils, and of homogeneous mixtures of refrigerant and flooding mediums.

2.2 Pre-conditioning and cycle solver

The individual components of the ORC system are connected together in a cycle model. The solution of a simulation is initialized with a pre-conditioner, which calculates the first set of guesses of the evaporating and condensing temperatures and other required parameters. The pre-conditioner is basically equivalent to the main cycle to be solved with simplified models for the plate heat exchangers and expander. After the pre-conditioning loop is completed, the main solver drives three residuals to zero using a multi-variable Newton-Raphson algorithm. Two of these residuals are an overall energy balance and a conservation of mass flow rate between the pump and expander. Pressure drops through the system lines and heat exchangers are neglected so a momentum balance residual is not needed. The general form of

[1]The ACHP website is at http://achp.sourceforge.net.

the overall energy balance, which also includes the flooding loop, is given by:

$$\dot{W}_{pp,r} + \dot{Q}_{ev,r} + \dot{W}_{pp,oil} + \dot{Q}_{ev,oil} - \dot{W}_{exp} - \dot{Q}_{cd,r} = 0 \quad (1)$$

The third residual is the total mass of refrigerant in the system. The user can select whether this residual is minimized directly, by specifying the total system charge, or indirectly, by specifying the condenser exit subcooling. The validations proposed in this paper are limited to the cases in which subcooling is imposed. Additional details regarding the solution scheme can be found in Ziviani et al. (2015b).

3. PLATE HEAT EXCHANGER MODEL

Only plate heat exchangers (PHEX) are considered in the current version because they are a common choice for waste heat recovery. The model is based on a moving-boundary approach and a validation is proposed for both evaporating and condensing streams.

3.1 Moving Boundary approach

An efficient moving-boundary algorithm is implemented to simulate the steady-state behavior of the heat exchangers. The model is based on the algorithm proposed by Bell et al. (2015). This model can accommodate evaporator and condenser duty, as well as cascade duty heat exchangers, in which phase-change occurs in both fluid streams. The model is robust and guarantees that the temperature profiles are physically-possible. The PHEX is modeled as a counterflow heat exchanger with two streams, i.e. hot and cold, separated by a wall. By imposing the inlet states of both streams and the geometric parameters, the algorithm determines the maximum possible heat transfer rate corresponding to 100% effectiveness. Then, the heat transfer rate is decreased due to internal pinch points, allowing for the possibility of phase change in both streams. The actual heat transfer rate is obtained iteratively by using a numerical solver with proper physical boundaries, i.e. the heat exchanger is divided into a number of zones corresponding to a phase, i.e. liquid, vapor or two-phase. The residual function to be driven to zero is given by,

$$r\left(\dot{Q}\right) = 1 - \sum_j w_j = 1 - \sum_j \frac{A_{req,j}}{A_h} \quad (2)$$

where w_j represents the j-fraction of the total heat exchanger length predicted from each zone. The correct solution is achieved once the sum of the length fractions of all the zones is equal to unity. The current model is suitable for sub-critical conditions only and the internal pressure drops are neglected. An extension has been added in the code with respect to Bell et al. (2015), to allow incompressible fluids, i.e. thermal oils, to be used as a heat source. In the solution process, if an incompressible fluid is selected, the algorithm excludes vapor and two-phase zones from the possible combinations by forcing the subcooled phase to be used. Thus, numerical artifacts have been added to eliminate the dependency on vapor quality.

4. EXPANDER MODEL

Different types of expander models have been included within the simulation frame: (i) an empirical model based on the Pacejka equation (for dry expansion only); (ii) a semi-empirical model based on the physics of the expander. Both models have been described and validated by the authors (Georges, 2012; Ziviani et al., 2015a) for a scroll and single-screw expanders under dry running conditions. In the following, the semi-empirical model is extended in order to allow for the liquid-flooded expansion process. The extension of the semi-empirical model to allow for liquid flooding, as well as the experimental data for a liquid-flooded scroll expander, were originally presented in (Georges, 2012). By considering the oil as an incompressible fluid and by assuming mechanical and thermal equilibrium between the refrigerant and the oil, the model is adapted by introducing a liquid fraction, i.e. ratio of the oil mass flow rate to the refrigerant mass flow rate, that accounts for different flooding ratios, $y_{oil} = \dot{m}_{oil}/\dot{m}_r$.

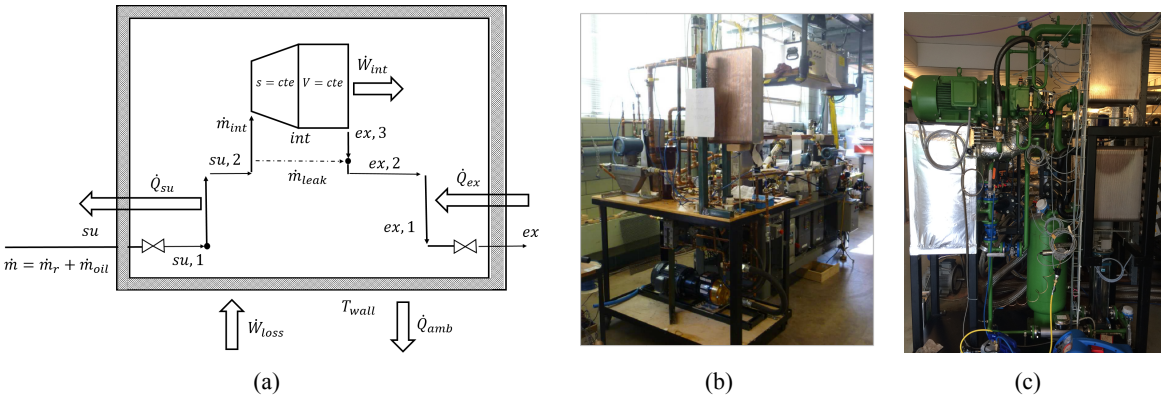

Figure 2: (a) Schematic of the semi-empirical model; (b) ORCLFE at Ray W. Herrick Laboratories, Purdue University; (c) ORC at UGent, Campus Kortrijk.

An effective built-in volume ratio, $r^*_{v,int}$, is defined due to the presence of oil in the expansion chamber:

$$r^*_{v,int} = \frac{r_{v,int} - a}{1 - a}, \tag{3}$$

where $a = \dot{V}_{oil,su}/\dot{V}_{dis,exp}$ is the fraction of the expander displacement volume that is occupied by oil. By considering the schematic proposed in Fig. 2(a), the expansion process is split into two steps, i.e. isentropic and constant volume, linked by a common internal state point. In particular, the isentropic step is computed by keeping the specific entropy of the mixture constant:

$$s_{m,int} = s_{m,su2} = s_{r,int} + x_{oil}\, s_{oil,int} = s_{r,int} + \left(\frac{\dot{m}_{oil}}{\dot{m}_r - \dot{m}_{leak}}\right) s_{oil,int} \tag{4}$$

where a new mass ratio, x_{oil}, has to be introduced to account for the internal leakage i.e. $\dot{m}_{r,int} = \dot{m}_r - \dot{m}_{r,leak}$ and the presence of oil. The internal isentropic work and the work at constant volume are expressed by:

$$\begin{aligned} w_{int,s} &= h_{r,su2} - h_{r,int} + x_{oil}\left(h_{oil,su2} - h_{oil,int}\right) \\ w_{int,V} &= \left(p_{r,int} - p_{r,ex2}\right)\left(v_{r,int} + x_{oil} v_{oil,su2}\right) \end{aligned} \tag{5}$$

The overall definition of the isentropic effectiveness is then given by:

$$\epsilon_{exp,s} = \frac{\dot{m}_{r,int}\left(w_{int,s} + w_{int,V}\right) - \dot{W}_{loss}}{\dot{m}_r\left[h_{r,su} - h_{r,ex,s} + y_{oil}\left(h_{oil,su} - h_{oil,ex,s}\right)\right]}, \tag{6}$$

where the mechanical losses $\dot{W}_{loss}$ are computed in the model as described in Ziviani et al. (2015a).

5. ORCSIM VALIDATION

The validation of the simulation tool has been carried out by considering two different ORC systems, shown in Fig. 2. The first one, Fig. 2(b), is an ORC with liquid-flooded expansion and internal regeneration (ORCLFE), where the high pressure and temperature refrigerant is homogeneously mixed before entering the expander with a lubricant oil at the same thermodynamic conditions in order to force the expansion toward a quasi-isothermal transformation. The working fluid is R134a and the lubricant oil is a 150 SUS polyol ester (POE) oil. The system includes four PHEXs (evaporator, oil heater, condenser and regenerator), two diaphragm pumps, a mixing section, an oil separator and a scroll expander (Woodland et al., 2013; Georges, 2012). Steam at around 105 °C and municipal water at around 15 °C are used as the hot and cold source, respectively. From the experimental results and data processing, 7 steady-state points have been obtained for different flooding ratios ($y_{oil} = 0 \sim 1$) with the rotational speed of the expander fixed at 2500 rpm, as reported in (Georges, 2012). The second system, Fig. 2(c),

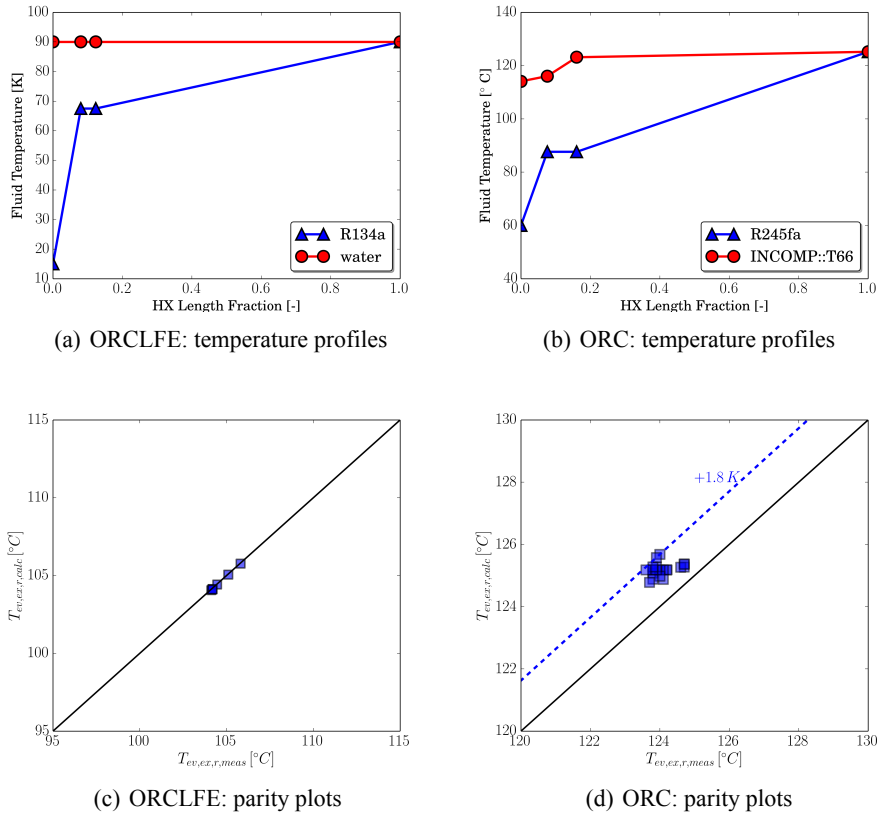

(a) ORCLFE: temperature profiles

(b) ORC: temperature profiles

(c) ORCLFE: parity plots

(d) ORC: parity plots

Figure 3: Validation of the PHEX model in the case of the evaporators.

is a standard ORC with regenerator derived from an industrial version. The system is composed of three identical PHEXs, a multi-stage turbopump, a liquid receiver and an 11 kW single-screw expander. The working fluid is R245fa. A thermal oil, therminol 66 (or simply T66), is used as the heat source. It is heated by means of a 250 kWe electric heater. Typical supply temperatures of the T66 are around 125 °C. The cooling medium is a mixture of water and ethylene glycol (around 30% by volume), which is cooled by a rooftop air-cooler unit. A total of 60 steady-state points have been identified at different expander rotational speeds (Ziviani et al., 2015a). Only the nominal speed of 3000 rpm is considered for the following validation, i.e. 21 steady-state points. The first part of the validation addresses the PHEX and expander components for each of the ORC systems. The second part is related to the overall cycle model and the estimation of the cycle efficiency.

5.1 Validation of PHEX model as evaporator

The validation of the moving-boundary model applied to the evaporators is carried out by imposing the mass flow rate and the inlet temperature and pressure of the heat source fluid and the refrigerant. The model is used to determine the heat transfer rate and the outlet temperatures. The first result that is possible to obtain is the temperature profile across the heat exchanger length for both streams. Fig. 3(a) shows the temperature profile in the case of the ORCLFE, where the hot stream is saturated steam and the working fluid is R134a. Similarly, Fig. 3(b) represents the temperature profile in the case of the standard ORC with T66 as the heat source fluid and R245fa as the working fluid. Note that the internal location of phase-change points is predicted by the model. In a design-stage analysis, this information would allow one to optimize the geometry of the evaporators. The parity plots of the calculated outlet temperature of the refrigerant, $T_{ev,ex,r,calc}$, with respect to the experimental data, $T_{ev,ex,r,meas}$, are shown in Fig. 3(c) and Fig. 3(d). In particular, Fig. 3(c) represents the outlet temperature for the evaporator installed in the ORCLFE. The relative error between calculated and measured values is negligible. This is due to the high heat capacity of the steam relative to the working fluid. It results in the limiting case

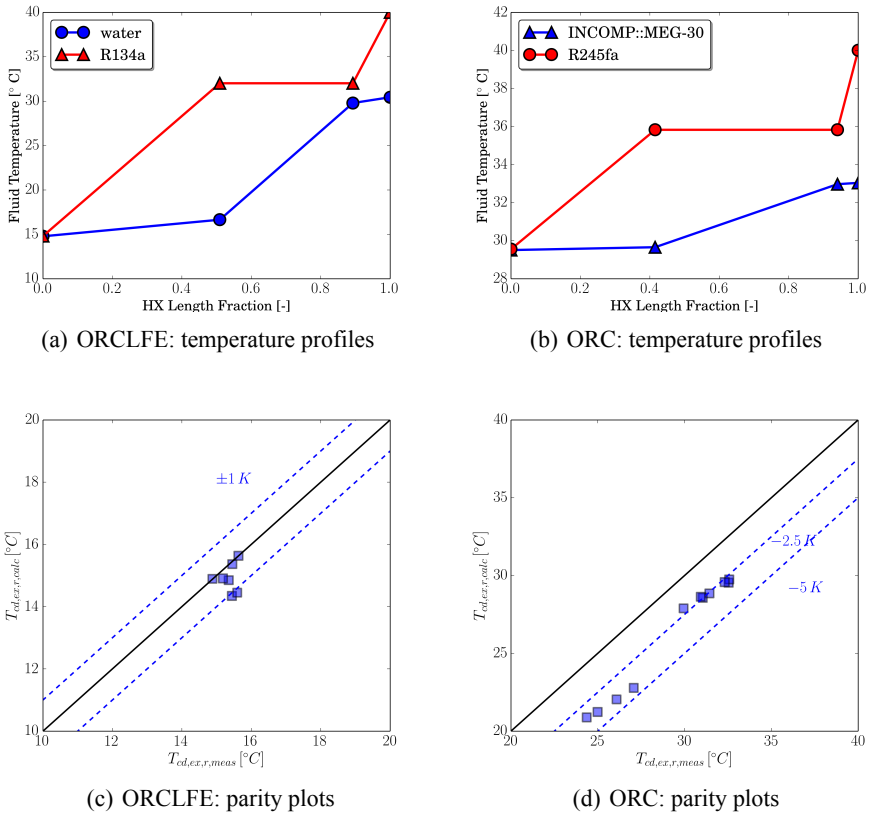

(a) ORCLFE: temperature profiles

(b) ORC: temperature profiles

(c) ORCLFE: parity plots

(d) ORC: parity plots

Figure 4: Validation of the PHEX model in the case of the condensers.

that the working fluid exit temperature is equal to the steam inlet temperature. In the case of the standard ORC with R245fa and T66 (Fig. 3(b)), the maximum heat transfer case is also apparent. However, the outlet temperature of the refrigerant is actually over-predicted by up to 1.8 K. A comparison between the thermo-physical property routines CoolProp and REFPROP has also been done in terms of computational time. By considering a single run of the PHEX model in the case of R134a and steam steady-state points, the same calculation has been performed using CoolProp, REFPROP called through CoolProp and native REFPROP. The PHEX simulation with CoolProp resulted to be 1.44 times faster than native REFPROP and up to 9.63 times faster than using CoolProp as an interface layer to REFPROP.

5.2 Validation of the PHEX model as condenser

In the same manner as for the evaporators, the PHEX model has been applied to the condensers by imposing the mass flow rate of both streams and the inlet conditions. For each of the ORC systems, two examples of the temperature profiles across the PHEX length and the parity plots of the outlet temperature of the refrigerant calculated and measured, $T_{cd,ex,r,calc}$ and $T_{cd,ex,r,meas}$, are shown in Fig. 4(c). It should be noted that the ORCLFE uses water as the cooling medium, while the standard ORC has an aqueous mixture of ethylene glycol. The outlet temperatures have been predicted within 1 K and 2.5 K, respectively. Only four points in the case of R245fa/ethylene glycol aq. have been predicted within 5 K. This represents an error in the predicted heat transfer rate of 11 %. The same results have been obtained with native REFPROP. In the current PHEX model, general heat transfer correlations are implemented in order to guarantee a general validity. An improvement could be made by integrating refrigerant-specific heat transfer correlations.

5.3 Validation of the expander model

The semi-empirical model proposed for the expanders aims to be general enough to cover different types of positive displacement machines and different operating conditions by adjusting a set of parameters.

As mentioned before, two different expanders have been considered in this study, i.e. a scroll expander with liquid-flooded expansion and a single screw expander. The model has been calibrated with the experimental points of each machine by means of a genetic algorithm. The procedure is explained in Ziviani et al. (2015a). It should be noted that the limited number of steady-state points obtained for the scroll expander under different flooding ratios does not allow for a validation of the model over a wide range of operating conditions. Nevertheless, it is possible to verify whether the model is able to capture the influence of the flooding medium. Regarding the single screw expander, a more comprehensive investigation and analysis of such a machine can be found in Ziviani et al. (2015a). The comparison between experimental data and calculated results is carried out by providing the expander rotational speed, inlet pressure and temperature, the expander discharge pressure and the ratio of the oil to the refrigerant mass flow rate. In the case of the single screw expander, the last parameter is set to zero. The result of the validation is a set of parity plots for the predicted refrigerant mass flow rate, the power output, the discharge temperature and the adiabatic efficiency. The validation of the scroll expander is shown in Fig. 5. Fig. 6 shows the four parity plots for the single screw expander. By comparing the results of both expanders, it is possible to notice that the model presents a better agreement in the case of the single screw expander, mainly because the complexity of two-phase, two-component flow within the working chamber is not involved. Despite this added complexity with the liquid-flooded scroll expander, the model is able to predict its performance with reasonable accuracy. Note that, while the mass flow rate is overestimated in all of the cases within 10% (Fig. 5(a)), the discharge temperature agrees within 1 K (Fig. 5(c)). The power output presents a larger deviation compared to the previous parameters, as shown in Fig. 5(b). The predictions have been improved by using a compressible two-phase flow model to calculate the pressure drop at the inlet port of the expander, as proposed by Morris (1991). The remarked difference between the measured and the predicted power is related to the presence of the oil and the consequent mechanical losses. The viscous effect of the oil increases with the flooding ratio. A proper viscosity model to take into account these losses should be introduced. The uncertainties of mass flow rate and power output within the model accumulate and directly affect the predictions of the adiabatic efficiency, as shown in Fig. 5(d).

5.4 Overall cycle validation

ORCSim is used to validate the cycle models of the ORCLFE and the standard ORC. The general definition of the cycle thermal efficiency for the ORC with liquid-flooded expansion is given by,

$$\eta_{ORCLFE} = \frac{\dot{W}_{exp} - \dot{W}_{pp,r} - \dot{W}_{pp,oil}}{\dot{Q}_{ev} + \dot{Q}_{oil}} \tag{7}$$

The definition is readily adapted for the standard ORC by dropping the terms related to the oil loop. The cycle simulations have been performed by using the condenser exit subcooling as a convergence criteria (in addition to the cycle mass flow and energy balances). Two examples of temperature-entropy plots of the cycle are shown in Fig.7 for both the ORCLFE and the standard ORC. For most of the points of the ORCLFE, the error on the prediction of the cycle efficiency is less than 25%. Higher accuracy has been obtained in the case of the standard ORC for several points. The parity plots are shown in Fig. 8.

6. CONCLUSIONS

In this paper, a general ORC simulation framework is presented. The architecture of the software has been described and its capabilities have been proven by considering two cycle architectures: an organic Rankine cycle with liquid-flooded expansion (ORCLFE) and internal regeneration using R134a with a scroll expander and a traditional ORC system using R245fa as working fluid with a single screw expander. The main results achieved are summarized below.

- A moving boundary model has been used to model PHEX. The model is general and it is able to capture the performance of an evaporator, a condenser or a regenerator. Thus, a wide range of

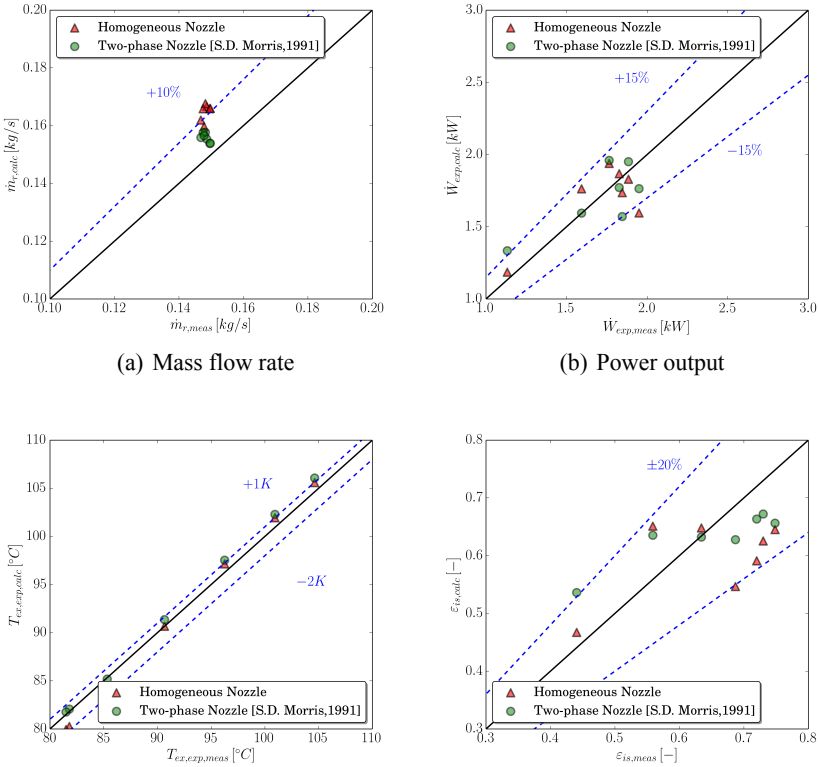

(a) Mass flow rate (b) Power output

(c) Discharge temperature (d) Isentropic efficiency

Figure 5: Scroll expander parity plots.

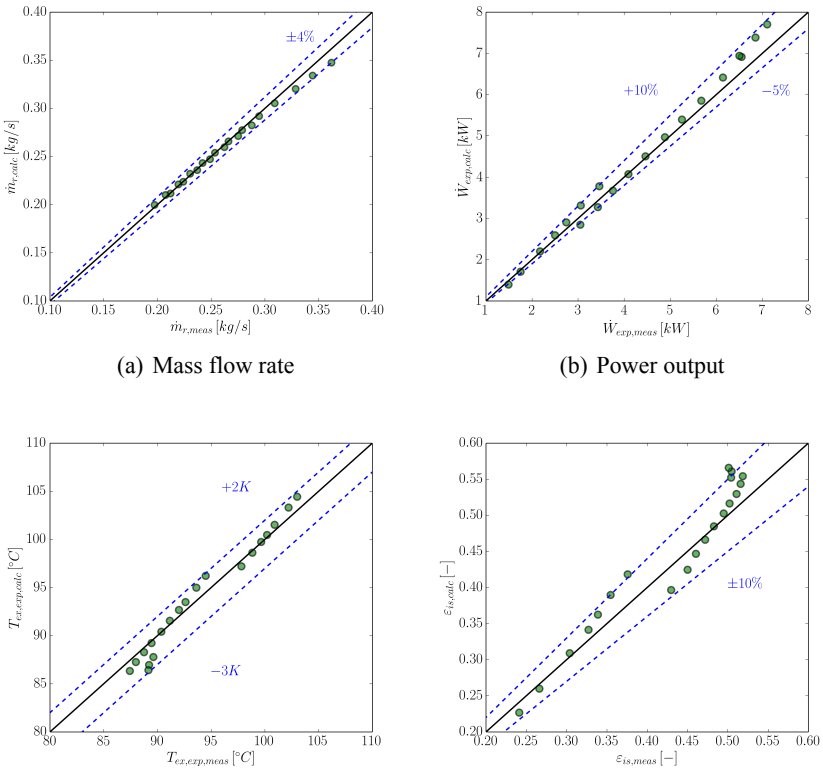

(a) Mass flow rate (b) Power output

(c) Discharge temperature (d) Isentropic efficiency

Figure 6: Single screw expander parity plots.

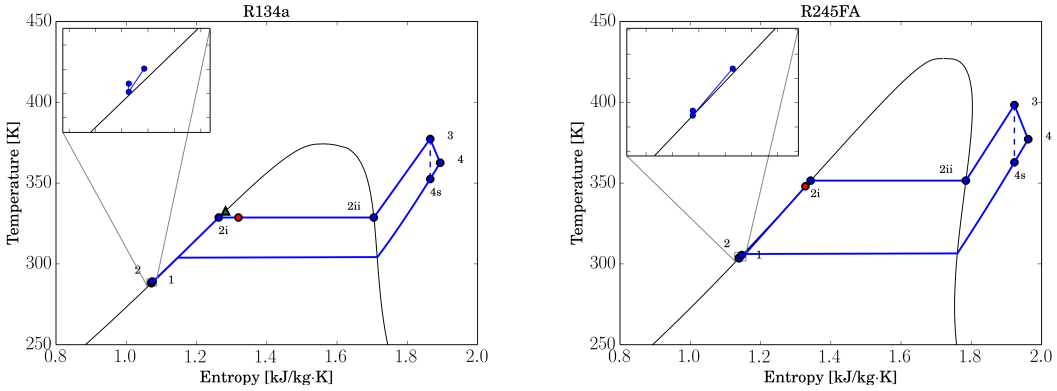

(a) y_{oil}= 0.26, $T_{exp,out}$= 90 °C (b)

Figure 7: T-s diagram: (a) ORCLFE;(b) standard ORC.

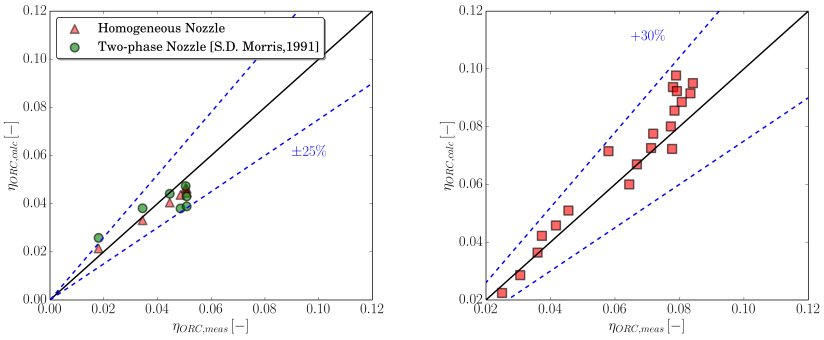

(a) (b)

Figure 8: (a) ORCLFE cycle efficiency;(b) ORC cycle efficiency.

fluids, i.e. refrigerants, incompressible liquids, mixtures, etc., have been included. The model has been validated as an evaporator and a condenser for both ORC systems.

- A general semi-empirical model of an expander has been implemented to take into account the presence of different oil fractions. The model has been calibrated for two different expanders, i.e. scroll and single screw, showing good agreement with the experimental results. The agreement is not as good for the liquid-flooded scroll expander. Additional data and more model sophistication could yield improved results. The validation has been shown with a set of parity plots for mass flow rate, power output, discharge temperature and adiabatic efficiency.
- The validation of the overall cycle performance in terms of thermodynamic efficiency has also been carried out. The maximum relative error of 25.7% was obtained in the case of the ORCLFE. This is attributed to the fact that both fluids enter the evaporator in the two-phase state, making heat input measurement highly uncertain. Also, several uncertainties can be associated with the presence of oil in the expander model. For the ORC, the maximum relative error on efficiency prediction was 28.9% mainly because of the over estimation of the expander power output.

REFERENCES

Bell, I. H., Quoilin, S., Georges, E., Braun, J. E., Groll, E. A., Horton, W. T., and Lemort, V. (2015). A generalized moving-boundary algorithm to predict the heat transfer rate of counterflow heat exchangers for any phase configuration. *Applied Thermal Engineering*, 79:192--201.

Bell, I. H., Wronski, J., Quoilin, S., and V, L. (2014). Pseudo-pure fluid thermophysial property evalu-

ation and the open-source thermophysical property library coolprop. *Ind. Eng. Chem. Res.*, 53:2498--2508.

Georges, E. (2012). Investigation of a flooded expansion organic rankine cycle system. Master's thesis, University of Liege.

Lemmon, E. W., Huber, M. L., and McLinden, M. O. (2013). Nist standard reference database 23: Reference fluid thermodynamic and transport prop-erties-refprop, version 9.1. National Institute of Standards and Technology, Standard Reference Data Program, Gaithersburg.

Morris, S. D. (1991). Compressible gas-liquid flow through pipeline restrictions. *Chem. Eng. Process.*, 30:39--44.

Quoilin, S., Lemort, V., and Lebrun, J. (2010). Experimental study and modeling of an organic rankine cycle using scroll expander. *Applied Energy*, 87:1260--1268.

Woodland, B. J., Braun, J. E., Groll, E. A., and Horton, W. T. (2014). Methods of increasing net work output of organic rankine cycles for low-grade waste heat recovery. In *15th Int.Refrigeration and Air Conditioning Conf. at Purdue*, number 2190.

Woodland, B. J., Krishna, A., Groll, E. A., Braun, J. E., Horton, W. T., and Garimella, S. V. (2013). Thermodynamic comparison of organic rankine cycles employing liquid-flooded expansion or a solution circuit. *Applied Thermal Engineering*, 61:859--65.

Ziviani, D., Desideri, A., Lemort, V., De Paepe, M., and van den Broek, M. (2015a). Low-order models of a single-screw expander for organic rankine cyle applications. In *9th Int. Conf. on Compressors and their Systems, City University of London, London*, number 38.

Ziviani, D., Woodland, B. J., Georges, E., Groll, E. A., Braun, J. E., Horton, W. T., De Paepe, M., and van den Broek, M. (2015b). Development of a general organic rankine cycle simulation tool: Orcsim. In *Proceedings of ECOS 2015: the 28th Int. Conf. on Efficiency, Cost, Optimization, Simulation and Environmental Impact of Energy Systems.*, number 50492.

NOMENCLATURE

A	area	(m^2)
h	specific enthalpy	(J/kg)
$\dot{m}$	mass flow rate	(kg/s)
p	pressure	(Pa)
$\dot{Q}$	heat rate	(W)
r_v	volume ratio	(-)
s	specific entropy	(J/kg-K)
T	temperature	(K)
v	specific volume	(m^3/kg)
$\dot{V}$	volume flow rate	(m^3/s)
w	specific work	(J/kg)
$\dot{W}$	power	(W)
x	mass ratio	(-)
y	mass ratio	(-)
ϵ	adiabatic efficiency	(-)
η	cycle efficiency	(-)

Subscript

cd	condenser
dis	displacement
ex	exhaust
exp	expander
ev	evaporator
h	hot side
int	internal
m	mixture
pp	pump
oil	flooding fluid (oil)
r	refrigerant
req	required
s	isentropic
su	supply

ACKNOWLEDGEMENT

The authors would like to acknowledge Ian H. Bell from NIST for his advice on numerous occasions regarding CoolProp and the Python programming language.